Particle size dependent electrophoresis in polymer solutions

Joseph Bentor and Xiangchun Xuan*

Department of Mechanical Engineering, Clemson University, Clemson, SC 29634-0921, USA

* Corresponding author. Email: xcxuan@clemson.edu (Dr. Xuan).

ABSTRACT

It has been long known that the electrophoretic velocity of a charged particle is independent of its size under the thin-Debye-layer limit. This so-called Smoluchowski velocity is, however, only valid for Newtonian fluids. A couple of recent theoretical studies predict the rheology-induced particle size dependence of electrophoresis in non-Newtonian fluids. This work presents the first experimental demonstration of such dependence in viscoelastic poly(ethylene oxide) (PEO) solutions. Three different-sized particles are observed to travel at the same electrophoretic velocity in a Newtonian buffer through a rectangular microchannel. In contrast, their measured electrophoretic velocities in the PEO solution exhibit an increasing trend for larger particles, which is consistent with the theoretical prediction. This particle size dependence is found to grow with increasing concentration or length of the PEO polymer. Both trends are attributed to the enhanced fluid elasticity as characterized by the increasing elasticity number.

INTRODUCTION

Electrophoresis is the movement of a charged particle with respect to a liquid electrolyte under an applied electric field.[1,2] It has found many applications ranging from DNA sequencing by capillary electrophoresis to cell manipulation in electrokinetic microfluidic devices.[3-6] The electrophoretic velocity of a moderately charged particle with $\sigma^* = \sigma a/\varepsilon\phi \sim 1$, where σ is the particle's surface charge density, a is the particle radius, ε is the liquid permittivity and ϕ is the thermal voltage, is a linear function of the imposed electric field strength, E, when $\beta = Ea/\phi \ll 1$.[7,8] This velocity follows Henry's formula and exhibits an explicit dependence on the particle size through $\delta = 1/\kappa a$ with $1/\kappa$ being the Debye length.[9,10] It reduces to Smoluchowski's formula under the thin-Debye-layer limit with $\delta \ll 1$, which becomes independent of the particle size and shape.[11] This regime of linear electrophoresis, however, breaks down for a highly charged particle with $\sigma^* \gg 1$ and/or under a large electric field with $\beta \gg 1$ because of the surface conduction effect in the Debye layer.[12-22] The resulting nonlinear contribution to the electrophoretic velocity has been demonstrated to depend on the size, charge and shape of the particle.[23-35] Particle size dependent electrophoretic velocity (more accurately, electrokinetic velocity because of the contribution of fluid electroosmosis) also occurs in a confined microchannel because of the boundary effect.[36,37] This dependence, however, remains insignificant unless the particle size-to-channel width ratio reaches the order of unity.[38,39]

The studies reviewed above are all concerned with particle electrophoresis in Newtonian fluids. Recent investigations have highlighted the significant impacts of fluid rheological

properties on various electrokinetic phenomena.[40-50] In particular, a couple of theoretical papers predict the onset of particle size dependent electrophoresis in non-Newtonian fluids even under the thin-Debye-layer limit. Khair et al.[51] developed a general framework to calculate the electrophoretic velocity of a uniformly charged colloidal particle immersed in a complex fluid with a shear-rate-dependent viscosity. They considered both a power-law and a Carreau fluid in their theoretical scheme. They demonstrated the fluid rheology, either shear thinning or thickening, can lead to an explicit particle size and shape dependence of electrophoresis because of the non-Newtonian stresses in the bulk fluid outside the thin Debye layer. In a later study, Li and Koch[52] analyzed the electrophoretic velocity of a weakly charged particle with a thin Debye layer in a dilute polymer solution. They modelled the polymer solution with different constitutive equations to account for the fluid elasticity and shear thinning effects. Their analysis indicates that the addition of polymers decreases the electrophoretic velocity because of both the increased viscosity and the induced fluid elasticity. The latter influence is manifested in terms of the Weissenberg number, $Wi = \lambda U/a$ where λ is the fluid relaxation time and U is the electrophoretic particle velocity in a Newtonian fluid, illustrating the size dependence of particle electrophoresis in a viscoelastic fluid. The authors further noted that the fluid shear thinning effect increases the electrophoretic velocity, consistent with the numerical simulations from Hsu and co-workers[53-55] for both spherical and rod-shaped particles in Carreau fluids.

We present in this work an experimental study of particle electrophoresis in viscoelastic polymer solutions through a rectangular microchannel. We test particles of three different

diameters that travel at an (nearly) identical electrophoretic velocity in the polymer-free Newtonian solution. Thus, any difference in the measured electrophoretic velocity of the three types of particles in the polymer solutions should be attributed to the polymer addition-induced fluid rheological effects. We also investigate how varying the concentration or length of polymers affects the electrophoretic velocity of different-sized particles. Moreover, we attempt to integrate the polymer concentration and length effects into one dimensionless plot to highlight the impact of fluid elasticity on particle-size dependent electrophoresis.

MATERIALS AND METHODS

Microchannel and Chemicals

The experiment was conducted using a microfluidic device constructed from polydimethylsiloxane through the standard photo and soft lithography techniques.[56] This device features a straight microchannel which is 2 cm long with a rectangular cross-section measuring 100 μm in width and 50 μm in depth. The particle solutions were prepared by mixing and re-suspending 3, 5 and 10 μm-diameter spherical polystyrene particles (Sigma-Aldrich) into 0.01 mM phosphate buffer (specifically, 0.00754 mM disodium phosphate and 0.00246 mM monosodium phosphate)-based poly(ethylene oxide) (PEO) (Sigma-Aldrich) solutions. The Debye length for this primarily uni-bivalent solution was estimated to be around $1/\kappa = 0.06$ μm,[9] much smaller than the diameter of the smallest 3 μm particle for which $\delta = 1/\kappa a = 0.04 \ll 1$. Therefore, all three particles used in this work can be safely viewed to satisfy the thin-Debye-layer limit. The concentration of each

type of particles was kept low (< 0.1% in volume fraction) to minimize the particle-particle interactions.

The impact of fluid elasticity on particle electrophoresis was investigated under two conditions: one is to fix the molecular weight of PEO polymer to $M_w = 2$ MDa while varying its concentration from 500 to 1000 and 2000 ppm, and the other is to fix the polymer concentration to $c = 1000$ ppm while varying the molecular weight from 1 to 2 and 4 MDa. The pure buffer solution, i.e., PEO free or $c = 0$, was also tested as a control experiment. We calculated the overlap concentration of PEO polymers from the expression of Graessley,[57] $c^* = 0.77/0.072{M_w}^{0.65}$, and obtained $c^* = 1346$, 858 and 547 ppm for $M_w = 1$, 2 and 4 MDa, respectively. In other words, our prepared PEO solutions are all in the dilute to semi-dilute regime with a negligible to weak shear thinning effect.[58] Their zero-shear-rate viscosities, η_0, are extracted from our previous papers.[49,59] Their relaxation times were estimated from the scaling formula,[60] $\lambda \propto {M_w}^{2.073} c^{0.65}$, using the experimentally measured $\lambda = 1.5$ ms for $c = 1000$ ppm and $M_w = 2$ MDa PEO solution.[61] Table 1 summarizes the rheological properties of our prepared PEO solutions.

Table 1. Rheological properties of the prepared PEO solutions.

M_w (MDa)	c (ppm)	c^* (ppm)	λ (ms)	η_0 (mPa·s)	El
1	1000	1346	0.36	1.6	0.17
2	500	858	0.96	1.8	0.52
2	1000	858	1.5	2.4	1.1
2	2000	858	2.4	4.1	3.0
4	1000	457	6.3	3.3	6.2

Experimental Techniques

DC electric fields were used to drive the prepared particle solutions through the microchannel. They were supplied by a high-voltage DC power source (Glassman High Voltage, Inc.) and spanned from 100 to 400 V/cm. The corresponding dimensionless electric field, $\beta = Ea/\phi$, was calculated to vary from 0.6 (for 3 μm particle at 100 V/cm) to 8 (for 10 μm particle at 400 V/cm). This range of β was found in our recent paper[30] to be not large enough to induce nonlinear electrophoresis for the same types of particles in the same Newtonian buffer solution as in this work. Joule heating effect was estimated negligible in 0.01 mM buffer-based solution over this range of electric fields.[30,62] The electrokinetic motion of particles was recorded in the middle of the microchannel using a microscope (Nikon Eclipse TE2000U, Nikon Instruments) equipped with a CCD camera (Nikon DS-Qi1Mc). It was observed to align with the electric field direction for each type of particles in the suspensions, indicating a stronger electroosmotic fluid flow than the opposing electrophoretic particle motion such that,

$$V_{ep} = V_{eo} - V_{ek}, \quad (1)$$

where V_{ep}, V_{eo} and V_{ek} are the magnitudes of electrophoretic, electroosmotic, and electrokinetic velocities, respectively. The value of V_{eo} in each of the particle-free PEO and buffer solutions was measured using the electric current monitoring technique[63] for the range of DC electric fields under test. The value of V_{ek} was determined using ImageJ software (National Institutes of Health) for

each type of particles traveling near the centerline of the microchannel. More than twenty particles were tracked in each analysis to obtain the average of V_{ek}.

RESULTS AND DISCUSSION

Particle Electrophoresis in a Newtonian and a Polymer Solution

Figure 1 shows the sequential images of the mixture of 3, 5 and 10 μm-diameter particles in the flow of Newtonian buffer (a) and 1000 ppm PEO ($M_w = 2$ MDa) (b) solutions, respectively, through the rectangular microchannel. The applied DC electric field was fixed at 200 V/cm in both cases. As viewed from the timelapses on top of the images, the electrokinetic motion of particles slows down in the PEO solution (Figure 1b) compared to that in the Newtonian solution (Figure 1a). This observation is consistent with our previous studies,[45,47,50] which can be attributed to the polymer contribution to the viscosity and the polymer-induced elasticity.[52] The electrokinetic velocity remains nearly independent of the particle size in the Newtonian solution because the lines tracking the positions of different particles exhibit a parallel alignment in Figure 1a. This observation is evidenced by the experimentally measured data for the electrokinetic velocity, V_{ek}, of the three types of particles that almost overlap in Figure 2a for every DC electric field ranging from 100 to 400 V/cm. This phenomenon is consistent with our recent observation of the same three types of particles in 0.075 mM phosphate buffer solution,[30] indicating that these particles have almost equal zeta potentials in Newtonian solutions under the thin-Debye-layer limit.[8,10] Also shown in Figure 2a is the experimentally measured electroosmotic velocity, V_{eo}, in the Newtonian

buffer. It is obvious that both V_{ek} and V_{eo} (hence the electrophoretic velocity, V_{ep}, from eq 1) exhibit a linear relationship with respect to the applied DC electric field in this Newtonian solution, which is consistent with our earlier studies[30,35] indicating the absence of nonlinear electrophoresis[21] over the range of electric fields under study here.

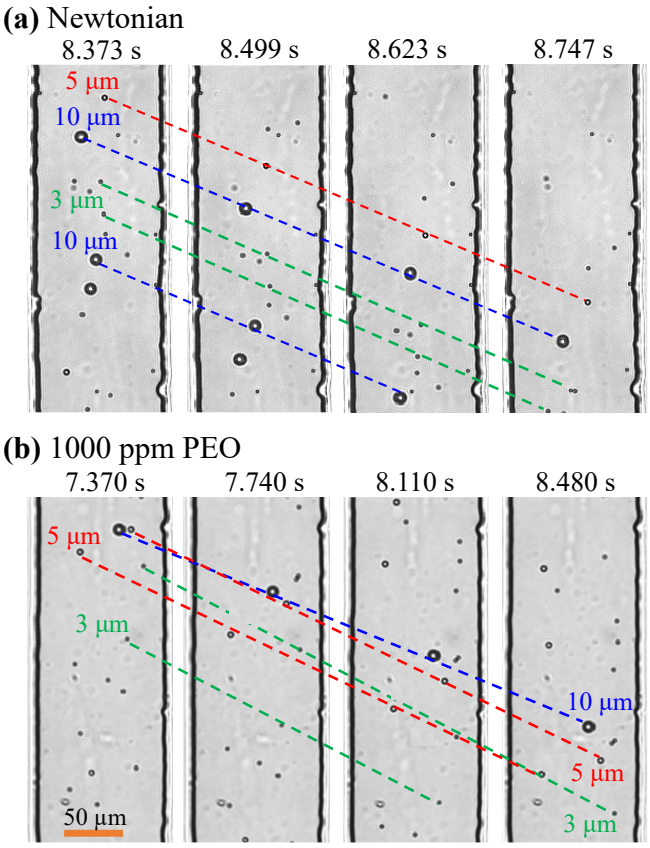

Figure 1. Sequential images illustrating the electrokinetic motion of 3, 5 and 10 μm-diameter particles in the Newtonian buffer (a) and 1000 ppm PEO (2 MDa, b) solutions through a rectangular microchannel under an applied electric field of 200 V/cm. The dashed lines track the particle positions as time (highlighted on top of the images) progresses.

In contrast, the slope of the particle tracking lines on the images in Figure 1b becomes steeper as the particle size decreases. Therefore, smaller particles have larger electrokinetic velocities in

the PEO solution, which is further demonstrate by the experimentally measured data of V_{ek} in Figure 2b for the DC electric field ranging from 100 to 400 V/cm. Also included in Figure 2b is the experimentally measured data for V_{eo} in the PEO solution over the same rage of DC electric fields. Like the observed trends for the Newtonian solution in Figure 2a, the obtained experimental data for V_{ek} and V_{eo} in the PEO solution can both be best fitted to linear trendlines in Figure 2b. This result suggests that the electrophoretic particle velocity, V_{ep} in eq 1, in the PEO solution also stays within the linear regime for the range of DC electric fields under test. Moreover, V_{ep} becomes smaller with the decrease of the particle diameter, which appears qualitatively consistent with the theoretical prediction of Li and Koch.[52] We are unable to perform a quantitative comparison of our experimental data with that theory as the latter is only valid for dilute polymer solutions with the polymer viscosity being much smaller than the solvent viscosity.[52] This assumption requires that the polymer concentration c be much lower than the overlap concentration c^*, which is not fulfilled in our experiment because the value of c/c^* is greater than 0.5 for all our prepared PEO solutions (see Table 1). The observed particle-size dependent electrophoresis should be related to the polymer-induced fluid elasticity because the only difference in the experimental conditions between Figure 2a and Figure 2b lies in the suspending medium. Specifically, this trend can be attributed to the increased deformation of polymers as they are electrokinetically advected around the smaller particles with a smaller radius of curvature.[52] We will present in the following sections a quantitative analysis of the parametric effects on particle size-dependent V_{ek} and V_{ep} in PEO solutions.

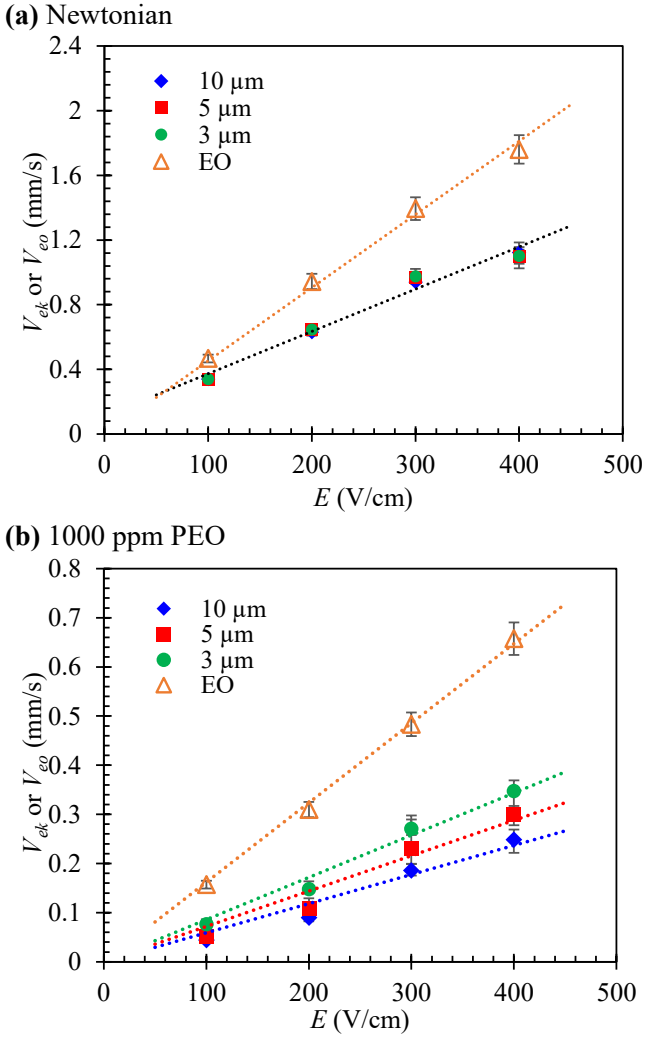

Figure 2. The experimentally measured electrokinetic velocity, V_{ek}, of 3, 5 and 10 µm-diameter particles and electroosmotic velocity, V_{eo}, in Newtonian buffer (a) and 1000 ppm PEO (2 MDa, b) solutions over a range of DC electric fields. The dashed lines are each a linear fit to the experimental data (symbols with error bars).

Effect of the Polymer Concentration

Figure 3 shows the experimental data for V_{ek} of 3, 5 and 10 µm-diameter particles and V_{eo} in 500 ppm (a) and 2000 ppm PEO ($M_w = 2$ MDa) (b) solutions over the range of DC electric fields from

100 to 400 V/cm. In comparison to 1000 ppm PEO in Figure 2b, we see a decrease in both V_{eo} and V_{ek} with the increase of the PEO concentration. This trend is consistent with our recent observation,[50] which, as noted above, should arise from the increased fluid viscosity and elasticity effect (see Table 1).[52] Moreover, we observe an intensified dependence of V_{ek} on the particle size as the PEO concentration increases from 500 ppm (Figure 3a) to 1000 ppm (Figure 2b) and 2000 ppm (Figure 3b). This trend is believed to be related to the stronger polymer deformation around a particle because of the increased presence of polymer strands therein as the polymer concentration gets higher.

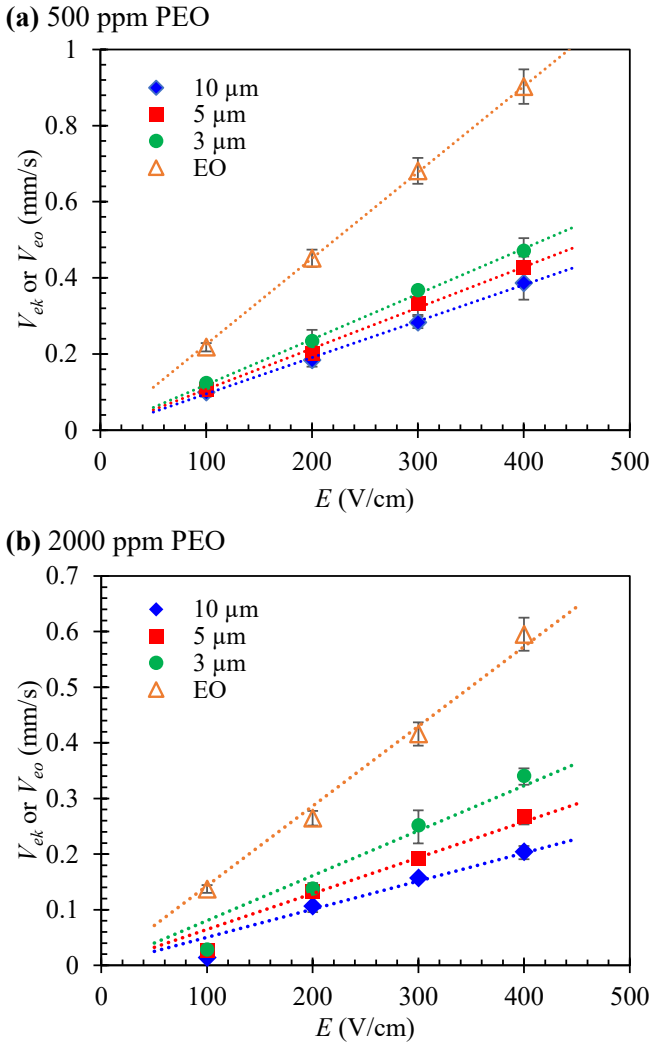

Figure 3. The experimentally measured electrokinetic velocity, V_{ek}, of 3, 5 and 10 µm-diameter particles and electroosmotic velocity, V_{eo}, in 500 ppm (a) and 2000 ppm PEO (2 MDa) (b) solutions over a range of DC electric fields. The dashed lines are each a linear fit to the experimental data (symbols with error bars).

In addition, we note that like 1000 ppm PEO solution in Figure 2b, V_{eo} and V_{ek} each exhibit a (almost) linear dependence on the DC electric field in 500 (Figure 3a) and 2000 ppm (Figure 3b) PEO solutions. Therefore, in the linear regime for electrokinetics, eq 1 can be rewritten as,

$$\mu_{ep} = \mu_{eo} - \mu_{ek}, \tag{2}$$

where μ_{ep}, μ_{eo}, and μ_{ek} are the so-called electrophoretic, electroosmotic and electrokinetic mobilities, respectively.[8,10] The values of μ_{eo} and μ_{ek} in the Newtonian and PEO solutions can each be obtained from the slopes of the linear trendlines to the experimental data for V_{eo} and V_{ek} in Figures 2 and 3. They are then used to determine the values of μ_{ep} from eq 2, which are presented in Figure 4 as a function of the particle diameter. The particle size dependence of μ_{ep}, and hence the electrophoretic velocity, V_{ep}, in the viscoelastic PEO solutions is clearly demonstrated in this figure. Moreover, though the absolute value of μ_{ep} for each size of particle decreases with the increase of the PEO concentration, their relative differences in fact become larger. This trend can be viewed from the equations displayed on the chart for the power trendline fit to the data points, indicating that μ_{ep} achieves a stronger dependence on the particle diameter in higher-concentration PEO solutions.

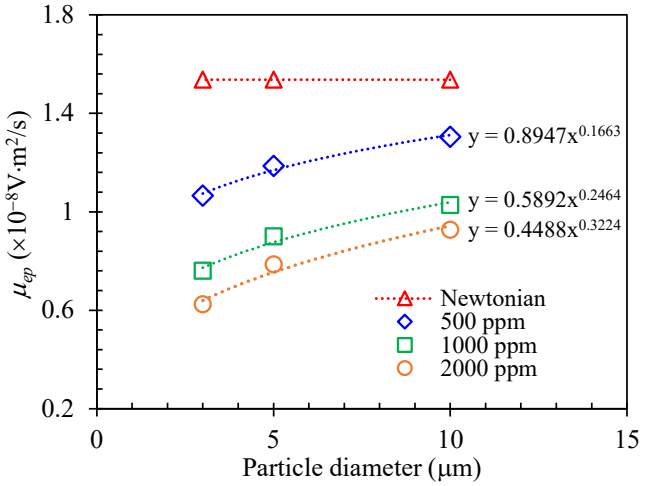

Figure 4. The experimentally obtained electrophoretic mobility, μ_{ep}, vs. the particle diameter in solutions with the concentration of PEO polymer (2 MDa) ranging from 0 (i.e., Newtonian) to 500,

1000 and 2000 ppm. The dashed lines are each a power trendline fit to the mobility data with the equation displayed on the chart.

Effect of the Polymer Length

Figure 5 shows the experimentally measured data for V_{ek} of 3, 5 and 10 μm-diameter particles and V_{eo} in 1000 ppm PEO solutions with $M_w = 1$ MDa (a) and 4 MDa (b), respectively, for the DC electric field ranging from 100 to 400 V/cm. Similar to the observed trends above in the PEO solutions with increasing polymer concentrations, we see a reduced V_{eo} and V_{ek} with the increase of M_w (or alternately the polymer length) from 0 (i.e., Newtonian, Figure 2a) to 1, 2 (Figure 2b) and 4 MDa. Moreover, the particle size dependence of V_{ek} becomes stronger with the increase of M_w because of the enhanced fluid elasticity effect. This trend is consistent with that when the PEO concentration is increased (see Figure 3) because longer-strand polymers experience a more pronounced deformation as they are advected around particles, particularly strong for particles with small radii of curvature.[52] It is important to note that there is an apparent deviation from the linear trendline for both V_{ek} and V_{eo} in 4 MDa PEO solution (Figure 5b). This phenomenon may be attributed to the fluid shear thinning effect that has been found to increase with the PEO length[58,64] and is expected to cause a more significant enhancement in both fluid electroosmosis and particle electrophoresis with the increase of the applied electric field.[40,53-55]

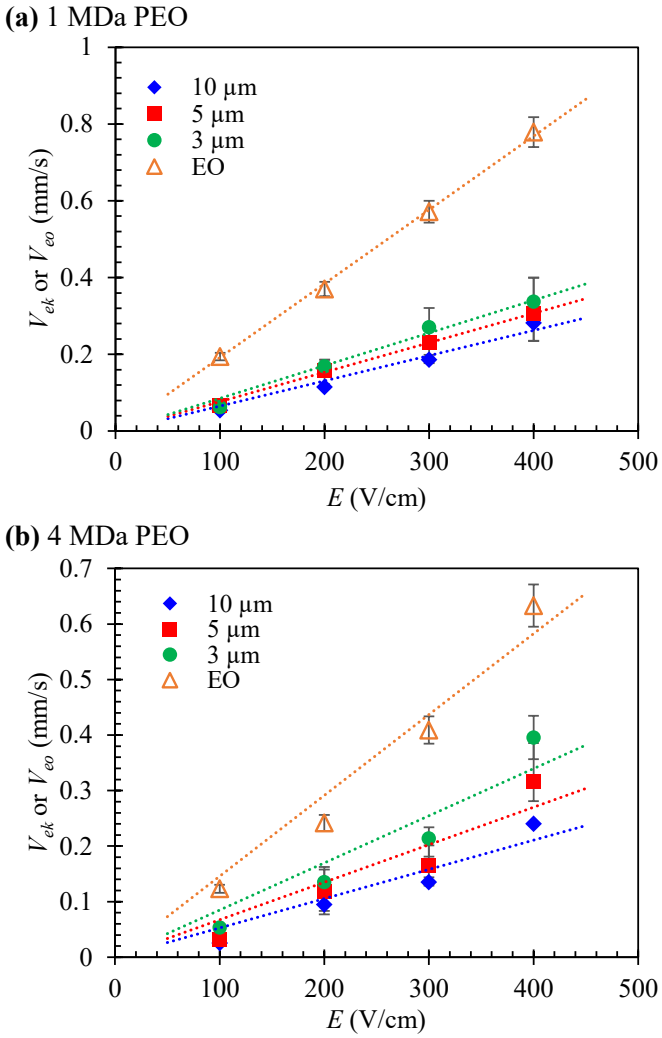

Figure 5. The experimentally measured electrokinetic velocity, V_{ek}, of 3, 5 and 10 µm-diameter particles and electroosmotic velocity, V_{eo}, in 1000 ppm PEO solutions with the molecular weights of 1 MDa (a) and 4 MDa (b) over a range of DC electric fields. The dashed lines are each a linear fit to the experimental data (symbols with error bars).

Like Figure 4, we used the slopes of the linear trendlines for V_{eo} and V_{ek} in Figure 5 to first obtain the values of μ_{eo} and μ_{ek} and then calculate the values of μ_{ep} from eq 2. It is admitted that this treatment may not be accurate for the 4 MDa PEO solution where nonlinearity starts appearing at higher electric fields. We will investigate in future work whether and how fluid shear thinning

impacts the electric field-driven fluid flow and particle motion. Figure 6 presents the obtained values of μ_{ep} of 3, 5 and 10 μm-diameter particles as a function of the M_w of PEO polymer (note: $M_w = 0$ indicates the Newtonian solution). Because of the increased fluid viscosity and elasticity (see Table 1), μ_{ep} decreases with the increase of M_w for each type of particles. However, this trend appears to slow down at higher values of M_w for all three particles, which may be because the total volume of polymers that are advected around any particles has an upper limit. The gap between μ_{ep} of any two pairs of particles still grows with the increase of M_w, indicating a stronger dependence of μ_{ep} on particle size in PEO solutions with longer polymer strands. This trend is consistent with that observed in the PEO solutions with increasing polymer concentrations (see Figure 4).

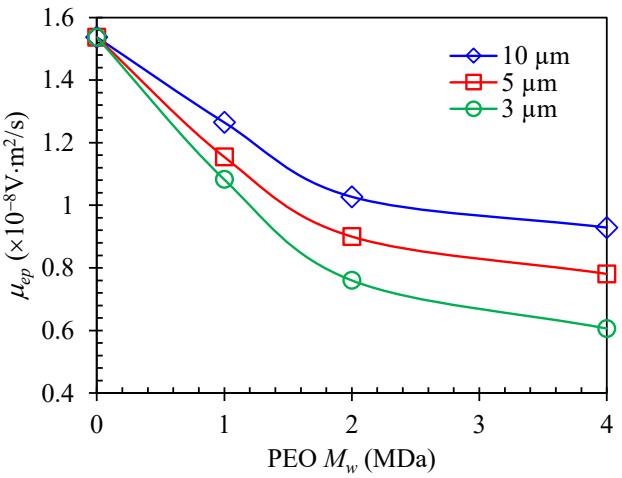

Figure 6. Effect of the molecular weight, M_w, of PEO polymer on the experimentally obtained electrophoretic mobility, μ_{ep}, of 3, 5 and 10 μm-diameter particles in Newtonian (i.e., $M_w = 0$) and 1000 ppm PEO solutions. The lines are used to guide the eyes only.

Summary of the Effect of Fluid Elasticity

To put together the results for the effects of polymer concentration and length into one plot for a unified understanding, we employ the so-called elasticity number, El, to characterize the fluid elasticity effect. This dimensionless number is defined as the ratio of the Weissenberg number to the Reynolds number and is independent of the fluid kinematics as given by,[50,58,61]

$$El = \frac{\lambda \eta_0 (w+h)}{\rho w^2 h}, \quad (3)$$

where the fluid relaxation time, λ, and viscosity, η_0, are both given in Table 1 for our prepared PEO solutions, ρ is the fluid density, and w and h are the width and height of the microchannel, respectively. As viewed from Table 1, increasing the concentration or molecular weight of the PEO polymer leads to a greater value of El. Figure 7 shows the ratios of μ_{ep} of 5 and 10 μm particles to that of 3 μm particles as a function of El in the prepared PEO and Newtonian solutions. For smaller values of El (less than 1), we observe a notably significant rise in both mobility ratios with the increase of El, signifying a substantial increase in the particle size dependence of μ_{ep}. Subsequently, there is a gradual ascent at higher values of El until a plateau seems to be reached at the highest value of $El \sim 6$ under test. This trend suggests that there may be a threshold value for El, beyond which no further enhancement in the particle size dependence of μ_{ep} can be observed. Such a phenomenon may be explained by the restriction posed upon the total volume of polymers that are advected around any particles with a limited space.

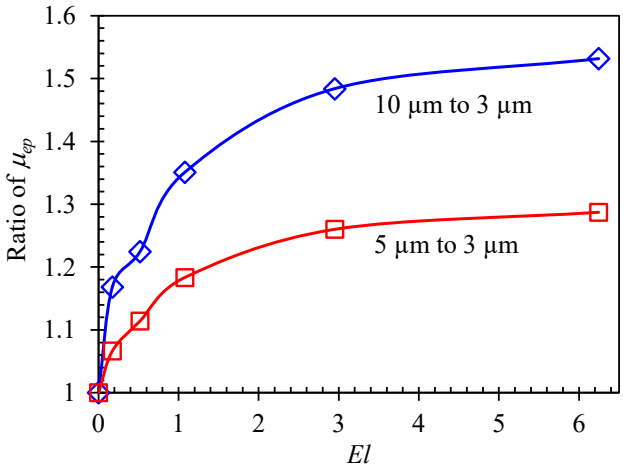

Figure 7. The ratios of the experimentally obtained electrophoretic mobility, μ_{ep}, of 5 and 10 μm-diameter particles to that of 3 μm particles as a function of the elasticity number, El. The lines are used to guide the eyes only.

CONCLUSIONS

We have experimentally demonstrated the fluid rheology-induced particle size dependence of electrophoretic velocity under the thin-Debye-layer limit. Smaller particles are observed to travel electrokinetically faster than larger ones in the viscoelastic PEO solution though all these particles travel at the same velocity in the Newtonian solution. The former observation indicates a larger electrophoretic velocity with increasing particle size, which is qualitatively consistent with the recent theoretical prediction of Li and Koch.[52] This phenomenon may be utilized to enhance the electrophoretic separation of micro/nanobioparticles in viscoelastic fluids for lab-on-a-chip applications. We have also conducted experiments to examine the effects of PEO concentration and length, respectively, on the electrophoretic mobility of particles in the linear regime of electric field. It is found that increasing either parameter leads to a stronger dependence of electrophoretic

velocity on the particle size, which can be integrated into one dimensionless plot in terms of the increasing elasticity number. This finding is expected to promote the use of electrophoresis for particle separation by size in microfluidic devices. We will investigate in future experiments whether and how fluid shear-thinning affects the electrophoretic behavior of particles.

ACKNOWLEDGEMENTS

This work was supported in part by NSF under grant numbers CBET-2100772 and CBET-2127825.

REFERENCES

[1] Hunter, R. J. *Zeta Potential in Colloid Science*. New York, Academic Press, 1981.

[2] Masliyah, J. H.; Bhattacharjee, S. *Electrokinetic and Colloid Transport Phenomena*. Hoboken, New Jersey, Wiley-Interscience, 2006.

[3] Kang, Y.; Li, D. Electrokinetic motion of particles and cells in microchannels. *Microfluid Nanofluid.* **2009**, *6*, 431-460.

[4] Zhao, C.; Yang, C. Advances in electrokinetics and their applications in micro/nano fluidics. *Microfluid Nanofluid.* **2012**, *13*, 179-203.

[5] Xuan, X. Recent advances in direct current electrokinetic manipulation of particles for microfluidic applications. *Electrophoresis* **2019**, *40*, 2484-2513.

[6] Song, Y.; Li, D.; Xuan, X. Recent advances in multi-mode microfluidic separation of particles and cells. *Electrophoresis* **2023**, *44*, 910-937.

[7] Lyklemma, J. *Fundamentals of Interface and Colloid Science*. Cambridge, MA, Academic Press, 1991.

[8] Li, D. *Electrokinetics in Microfluidics*. Burlington, MA, Elsevier Academic Press, 2004.

[9] Henry, D. C. The cataphoresis of suspended particles. Part I – the equation of cataphoresis. *Proc. R. Soc. Lond. A* **1931**, *133*, 106–129.

[10] Chang, H. C.; Yeo, L. Y. *Electrokinetically Driven Microfluidics and Nanofluidics*. New York, Cambridge University Press, 2010.

[11] Morrison, F. A. Electrophoresis of a particle of arbitrary shape. *J. Colloid Interface Sci.* **1970**, *34*, 210-214.

[12] O'Brien, R. W.; White, L. R. Electrophoretic mobility of a spherical colloidal particle. *J. Chem. Soc. Faraday Trans.* **1978**, *74*, 1607-1626.

[13] O'Brien, R. W. The solution of the electrokinetic equations for colloidal particles with thin double layers. *J. Colloid Interface Sci.* **1983**, *92*, 204-216.

[14] Mishchuk, N. A. Concentration polarization of interface and non-linear electrokinetic phenomena. *Adv. Colloid Interface Sci.* **2010**, *160*, 16-39.

[15] Schnitzer, O.; Yariv, E. Macroscale description of electrokinetic flows at large zeta potentials: nonlinear surface conduction. *Phys. Rev. E* **2012**, *86*, 021503.

[16] Schnitzer, O.; Zeyde, R.; Yavneh, I.; Yariv, E. Weakly nonlinear electrophoresis of a highly charged colloidal particle. *Phys. Fluids* **2013**, *25*, 052004.

[17] Dukhin, S. S. Electrophoresis at large peclet numbers. *Adv. Colloid Interface Sci.* **1991**, *6*, 219-248.

[18] Mishchuk, N. A.; Dukhin, S. S. Electrophoresis of solid particles at large Peclet numbers. *Electrophoresis* **2002**, *23*, 2012–2022.

[19] Shilov, V.; Barany, S.; Grosse, C.; Shramko, O. Field-induced disturbance of the double layer electro-neutrality and non-linear electrophoresis. *Adv. Colloid Interface Sci.* **2003**, *104*, 159–173.

[20] Schnitzer, O.; Yariv, E. Nonlinear electrophoresis at arbitrary field strengths: small-Dukhin-number analysis. *Phys. Fluids* **2014**, *26*, 122002.

[21] Khair, A. S. Nonlinear electrophoresis of colloidal particles. *Current Opinion Colloid Interface Sci.* **2022**, *59*, 101587.

[22] Cobos, R.; Khair, A. S. Nonlinear electrophoretic velocity of a spherical colloidal particle. *J. Fluid Mech.* **2023**, *968*, A14.

[23] Barany, S. Electrophoresis in strong electric fields. *Adv. Colloid Interface Sci.* **2009**, *147–148*, 36–43.

[24] Mishchuk, N. A.; Barinova, N. O. Theoretical and experimental study of nonlinear electrophoresis. *Colloid J.* **2011**, *73*, 88–96.

[25] Youssefi, M. R.; Diez, F. J. Ultrafast electrokinetics. *Electrophoresis* **2016**, *37*, 692-698.

[26] Tottori, S.; Misiunas, K.; Keyser, U. F. Nonlinear electrophoresis of highly charged nonpolarizable particles. *Phys. Rev. Lett.* **2019**, *123*, 014502.

[27] Cardenas-Benitez, B.; Jind, B.; Gallo-Villanueva, R. C.; Martinez-Chapa, S. O.; Lapizco-Encinas, B. H.; Pérez-González, V. H. Direct current electrokinetic particle trapping in insulator-based microfluidics: Theory and experiments. *Anal. Chem.* **2020**, *92*, 12871−12879.

[28] Antunez-Vela, S.; Perez-Gonzalez, V. H.; De Peña, A. C.; Lentz, C. J.; Lapizco-Encinas, B. H. Simultaneous determination of linear and nonlinear electrophoretic mobilities of cells and microparticles. *Anal. Chem.* **2020**, *92*, 14885–14891.

[29] Vaghef-Koodehi, A.; Dillis, C.; Lapizco-Encinas, B. H. High-resolution charge-based electrokinetic separation of almost identical microparticles. *Anal. Chem.* **2022**, *94*, 6451-6456.

[30] Bentor, J.; Dort, H.; Chitrao, R.; Zhang, Y.; Xuan, X. Nonlinear electrophoresis of dielectric particles in Newtonian fluids. *Electrophoresis* **2023**, *44*, 938-946.

[31] Ernst, O. D.; Vaghef-Koodehi, A.; Dillis, C.; Lomeli-Martin, A.; Lapizco-Encinas, B. H. Dependence of nonlinear electrophoresis on particle size and charge. *Anal. Chem.* **2023**, *95,* 6595–6602.

[32] Lomeli-Martin, A.; Ernst, O. D.; Cardenas-Benitez, B.; Cobos, R.; Khair, A. S.; Lapizco-Encinas, B. H. Characterization of the nonlinear electrophoretic behavior of colloidal particles in a microfluidic channel. *Anal. Chem.* **2023**, *95*, 6740−6747.

[33] Vaghef-Koodehi, A.; Ernst, O. D.; Lapizco-Encinas, B. H. Separation of cells and microparticles in insulator-based electrokinetic systems. *Anal. Chem.* **2023**, *95*, 1409−1418.

[34] Ahamed, N. N. N.; Mendiola-Escobedo, C. A.; Ernst, O. D.; Perez-Gonzalez, V. H.; Lapizco-Encinas, B. H. Fine-tuning the characteristic of the applied potential to improve AC-iEK separations of microparticles. *Anal. Chem.* **2023**, *95*, 9914−9923.

[35] Bentor, J.; Xuan, X.; Nonlinear electrophoresis of non-spherical particles in a rectangular microchannel. *Electrophoresis* **2024**, *45*, in press. https://doi.org/10.1002/elps.202300188

[36] Anderson, J. L.; Colloid transport by interfacial forces, *Annu. Rev. Fluid. Mech.* **1989**, *21*, 61–99.

[37] Keh, H. J.; Anderson, J. L.; Boundary effects on electrophoretic motion of colloidal spheres, *J. Fluid. Mech. 1985*, **153**, 417–439.

[38] Ye, C.; Li, D.; Electrophoretic motion of a sphere in a microchannel under the gravitational field. *J. Colloid Interface Sci.* **2002**, 251, 331-338.

[39] Xuan, X.; Raghibizadeh S.; Li, D.; Wall effects on electrophoretic motion of spherical polystyrene particles in a rectangular poly(dimethylsiloxane) microchannel. *J. Colloid Interface Sci.* **2006**, *296*, 743-748.

[40] Zhao, C.; Yang, C. Electrokinetics of non-Newtonian fluids: a review. *Adv. Colloid. Interface Sci.* **2013**, *201–202*, 94–108.

[41] Huang, Y.; Chen, J.; Wong, T. N.; Liow, J.-L. Experimental and theoretical investigations of non-Newtonian electro-osmotic driven flow in rectangular microchannels. *Soft Matt*. **2016**, *12*, 6206–6213.

[42] Mukherjee, S.; Das, S. S.; Dhar, J.; Chakraborty, S.; Das-Gupta, S. Electroosmosis of viscoelastic fluids: Role of wall Depletion layer. *Langmuir* **2017**, *33*, 12046–12055.

[43] Pimenta, F.; Alves, M. A. Electro-elastic instabilities in cross-shaped microchannels. *J. Non-Newton. Fluid Mech.* **2018**, *259*, 61–77.

[44] Bezerra, W. D. S.; Castelo, A.; Afonso, A. M. Numerical study of electro-osmotic fluid flow and vortex formation. *Micromachines* **2019**, *10*, 796.

[45] Ko, C. H.; Li, D.; Malekanfard, A.; Wang, Y.; Fu, L.; Xuan, X. Electroosmotic flow of non-Newtonian fluids in a constriction microchannel. *Electrophoresis* **2019**, *40*, 1387-1394.

[46] Sadek, S. H.; Pinho, F. T.; Alves, M. A. Electro-elastic flow instabilities of viscoelastic fluids in contraction/expansion micro-geometries. *J. Non-Newton. Fluid Mech.* **2020**, *283*, 104293.

[47] Bentor, J.; Malekanfard, A.; Raihan, M. K.; Wu, S.; Pan, X.; Song, Y.; Xuan, X. Insulator-based dielectrophoretic focusing and trapping of particles in non-Newtonian fluids. *Electrophoresis* **2021**, *42*, 2154-2161.

[48] Bentor, J.; Raihan, M. K.; McNeely, C.; Liu, Z.; Song, Y.; Xuan, X. Fluid rheological effects on streaming dielectrophoresis in a post-array microchannel. *Electrophoresis* **2022**, 43, 717-723.

[49] Li, D.; Xuan, X. Electro-elastic migration of particles in viscoelastic fluid flows. *Phys. Fluids* **2023**, *35*, 092013.

[50] Raihan, M. K.; Baghdady, M.; Dort, H.; Bentor, J.; Xuan, X. Fluid elasticity-enhanced insulator-based dielectrophoresis for sheathless particle focusing in very dilute polymer solutions. *Anal. Chem.* **2023**, *95*, 16013-16020.

[51] Khair, A. S.; Posluszny, D. E.; Walker, L. M. Coupling electrokinetics and rheology: Electrophoresis in non-Newtonian fluids. *Phys. Rev. E* **2012**, *85*, 016320.

[52] Li, G.; Koch, D. L. Electrophoresis in dilute polymer solutions. *J. Fluid Mech.* **2020**, *884*, A9.

[53] Lee, E.; Tsai, C. S.; Hsu, J.; Chen, C. J. Electrophoresis in a Carreau fluid at arbitrary zeta potentials. *Langmuir* **2004**, *20*, 7952–7959.

[54] Hsu, J. P.; Yeh, L. H.; Ku, M. H. Electrophoresis of a spherical particle along the axis of a cylindrical pore filled with a Carreau fluid. *Colloid Polym. Sci.* **2006**, *284*, 886–892.

[55] Yeh, L. H.; Hsu, J. P. Electrophoresis of a finite rod along the axis of a long cylindrical microchannel filled with Carreau fluids. *Microfluid. Nanofluid.* **2009**, *7*, 383–392.

[56] Zhu, J.; Xuan, X. Dielectrophoretic focusing of particles in a microchannel constriction using DC-biased AC electric fields. *Electrophoresis* **2009**, *30*, 2668-2675.

[57] Graessley, W. W. Polymer chain dimensions and the dependence of viscoelastic properties on concentration, molecular weight and solvent power. *Polymer* **1980**, *21*, 258−262.

[58] Wu, S.; Raihan, M. K.; Song, L.; Shao, X.; Bostwick, J. B.; Yu, L.; Pan, X.; Xuan, X. Polymer effects on viscoelastic fluid flows in a planar constriction microchannel. *J Non-Newton. Fluid Mech.* **2021**, *290*, 104508.

[59] Lu, X.; Xuan, X. Elasto-inertial pinched flow fractionation for continuous shape-based particle separation. *Anal. Chem.* **2015**, *87*, 11523-11530.

[60] Tirtaatmadja, V.; Mckinley, G. H.; Cooper-White, J. J. Drop formation and breakup of low viscosity elastic fluids: Effects of molecular weight and concentration. *Phys. Fluids* **2006**, *18*, 043101.

[61] Rodd, L. E.; Scott, T. P.; Boger, D. V.; Cooper-White, J. J.; McKinley, G. H. The inertio-elastic planar entry flow of low-viscosity elastic fluids in micro-fabricated geometries. *J. Non-Newtonian Fluid Mech.* **2005**, *129*, 1−22.

[62] Xuan, X. Review of nonlinear electrokinetic flows in insulator-based dielectrophoresis: From induced charge to Joule heating effects. *Electrophoresis* **2022**, *43*, 167–189.

[63] Sze, A.; Erickson, D.; Ren, L.; Li, D. Zeta-potential measurement using the Smoluchowski equation and the slope of the current-time relationship in electroosmotic flow. *J. Colloid Interface Sci.* **2003**, *261*, 402–410.

[64] Liu, C.; Ding, B.; Xue, C.; Tian, Y.; Hu, G.; Sun, J. Sheathless focusing and separation of diverse nanoparticles in viscoelastic solutions with minimized shear thinning. *Anal. Chem.* **2016**, *88*, 12547-12553.

FOR TABLE OF CONTENTS ONLY